Chemistry of Gene Silencing: The Mechanism of NAD$^+$-Dependent Deacetylation Reactions

Anthony A. Sauve,[‡] Ivana Celic,[§] Jose Avalos,[||] Haiteng Deng,[‡] Jef D. Boeke,*[,§] and Vern L. Schramm*[,‡]

Department of Biochemistry, Albert Einstein College of Medicine, 1300 Morris Park Avenue, Bronx, New York 10461, Department of Molecular Biology and Genetics and Department of Biophysics and Biophysical Chemistry, Johns Hopkins University School of Medicine, 725 North Wolfe Street, Baltimore, Maryland 21205-2185

Received September 28, 2001; Revised Manuscript Received October 22, 2001

ABSTRACT: The Sir2 enzyme family is responsible for a newly classified chemical reaction, NAD$^+$-dependent protein deacetylation. New peptide substrates, the reaction mechanism, and the products of the acetyl transfer to NAD$^+$ are described for SIR2. The final products of SIR2 reactions are the deacetylated peptide and the 2′ and 3′ regioisomers of *O*-acetyl ADP ribose (AADPR), formed through an α-1′-acetyl ADP ribose intermediate and intramolecular transesterification reactions (2′ → 3′). The regioisomers, their anomeric forms, the interconversion rates, and the reaction equilibria were characterized by NMR, HPLC, ^{18}O exchange, and MS methods. The mechanism of acetyl transfer to NAD$^+$ includes (1) ADP ribosylation of the peptide acyl oxygen to form a high-energy *O*-alkyl amidate intermediate, (2) attack of the 2′-OH group on the amidate to form a 1′,2′-acyloxonium species, (3) hydrolysis to 2′-AADPR by the attack of water on the carbonyl carbon, and (4) an SIR2-independent transesterification equilibrating the 2′- and 3′-AADPRs. This mechanism is unprecedented in ADP-ribosyl transferase enzymology. The 2′- and 3′-AADPR products are candidate molecules for SIR2-initiated signaling pathways.

The SIR2-like enzymes are broadly conserved from bacteria to humans (*1*, *2*). In yeast, these proteins form complexes with other proteins to silence chromatin (*3*−*6*) by accessing histones (*7*, *8*) and deacetylating them (*9*−*12*). Sir2 enzymes are homologues of the bacterial enzyme cobB, a phosphoribosyltransferase (*13*), and employ NAD$^+$ as a cosubstrate in deacetylation reactions (*10*, *12*, *14*). This requirement for NAD$^+$ is stoichiometric (*14*) and generates a novel product originally proposed to be β-1′-AADPR[1] (*15*, *16*) or possibly 2′-AADPR (*16*, *17*). From mechanistic and thermodynamic considerations, the NAD$^+$-dependent deacetylation by SIR2 is an unusual reaction, because lysine N-deacetylation reactions are simple to accomplish by hydrolysis alone. The apparent coupling of hydrolysis and ADP-ribose transfer to acetate forms a new metabolite of unknown function (*15*−*17*). The mechanism of Sir2 is reported here, together with unambiguous identification of the reaction products. This information furnishes insight into the chemical principles of SIR2-catalyzed deacetylation and permits a mechanistic interpretation of the X-ray crystal structure (*18*).

* To whom correspondence be addressed. E-mail: (J.B.) jboeke@jhmi.edu, (V.S.) vern@aecom.yu.edu. Phone: (718) 430-2813. Fax: (718) 430-8565.

‡ Albert Einstein College of Medicine.

§ Department of Molecular Biology and Genetics, Johns Hopkins University School of Medicine.

|| Department of Biophysics and Biophysical Chemistry, Johns Hopkins University School of Medicine.

[1] Abbreviations: AADPR, acetyl adenosine diphosphate ribose; ADPR, adenosine diphosphate ribose; ADP ribosylation, adenosine diphosphate ribosylation; NAD$^+$, nicotinamide adenine dinucleotide; SIR2, silent information regulator 2; SIR2Af2, SIR2 from thermophilic *Archaeoglobus fulgidus*.

Sir2 enzymes within species have multiple homologues (*1*), and the genomes of eubacteria such as *Salmonella* lack histones but encode Sir2-like proteins (*19*), suggesting broader substrate specificity for this family of enzymes. We examined the SIR2 reaction with p53 (*20*−*24*) and derived acetylated peptides and showed them to be competent substrates for the SIR2 deacetylation reaction. Reaction products were characterized by NMR, mass spectrometry, and isotopic exchange and were compared to chemical standards of expected products for the reaction. Reaction products are the deacetylated peptide, nicotinamide, and an acetyl-transfer product, 2′-AADPR. Solvent water ^{18}O incorporation established the uptake of one oxygen in the enzymatic reaction followed by a second ^{18}O exchange in acidic solution. Peptide deacetylation is coupled to an obligatory ADP ribosylation of the acetylated peptide substrate. The AADPR products of the reaction are new molecules to cellular pathways and are candidates for novel pathways of metabolism or signaling.

RESULTS

Chemical Synthesis of β-1′-AADPR. The AADPR product of the SIR2 reaction with NAD$^+$ and KKGQSTSRHKKA-cLMFKTEG (JB12) has the mass expected for β-1′-AADPR, but the same mass is also expected for 2′-AADPR and 3′-AADPR (*15*, *16*). The retaining glycohydrolase CD38 was used to synthesize β-1′-AADPR from NAD$^+$ in the presence of NAD$^+$ and 4 M sodium acetate at pH 6.5 (Figure 1A; *25*). An HPLC and NMR comparison of standard β-1′-AADPR to the AADPR product of SIR2 showed that the two compounds were different (see NMR data in Figure 2). The difference was confirmed by MS/MS studies, showing

10.1021/bi011858j CCC: $20.00
Published on Web 12/01/2001

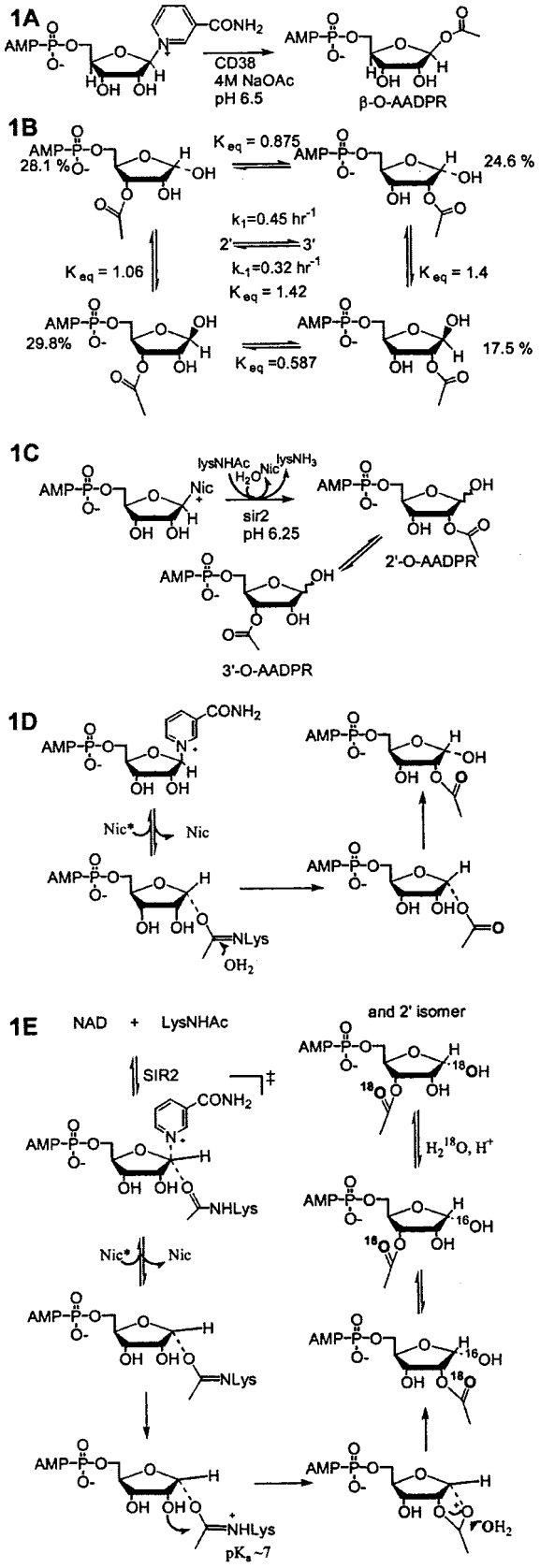

FIGURE 1: (A) CD38-catalyzed synthesis of β-1′-AADPR. (B) Observed equilibria of 2′-substituted and 3′-substituted α- and β-AADPRs and relative equilibrium populations at 15 °C. (C) Reaction sequence from NAD^+ in SIR2-catalyzed deacetylations. (D) ADP-ribosylation-dependent deacetylation to generate α-1′-AADPR with migration to 2′-AADPR. (E) NAD^+-dependent SIR2-catalyzed deacetylation mechanism generating 2′-AADPR, 3′-AADPR, and ^{18}O-labeled products.

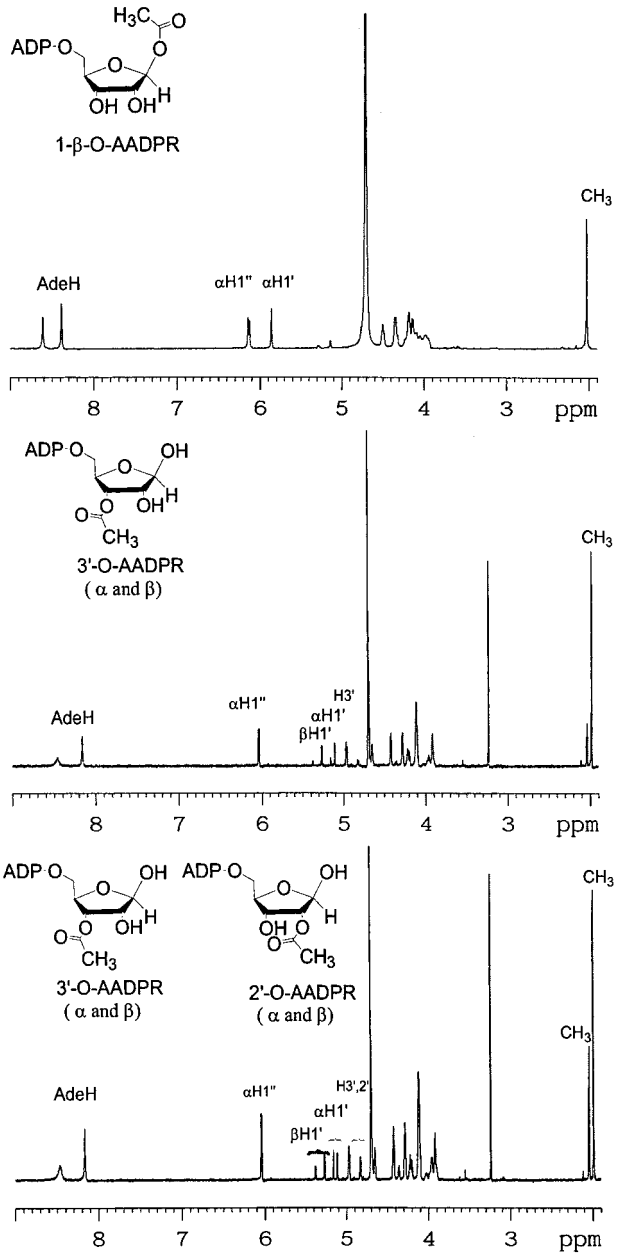

FIGURE 2: (Top panel) ^1H NMR of β-1′-AADPR in D_2O (300 MHz). (Middle panel) ^1H NMR of 3′-AADPR at 15 °C in D_2O (600 MHz). (Bottom panel) Sample from middle panel aged for several hours at 20 °C (600 MHz), showing an equilibrium of 2′- and 3′-AADPR isomers.

that the fragmentation patterns of the SIR2 product and β-1′-AADPR differed (Figure 3), although their masses were identical (see Methods).

Characterization of 2′- and 3′-AADPR from SIR2 Reactions. The SIR2 reaction produced two ADP-ribosyl acetate species by MS and HPLC analysis. The ^1H NMR of the SIR2 product eluting first by HPLC differed from that of β-1′-AADPR, although the acetate moiety is determined to be present on the basis of a methyl resonance at 2.1 ppm (Figure 2, top and bottom panels). When this sample was reanalyzed after refrigeration overnight, the ^1H NMR spectrum changed. The minor peaks (Figure 2, middle panel) became more fully developed (Figure 2, bottom panel), and subsequent spectra indicated that a stable ratio of peaks had been established. HPLC analysis yielded again the two peaks absorbing at 260 nm. Analysis by MS and MS/MS confirmed that both

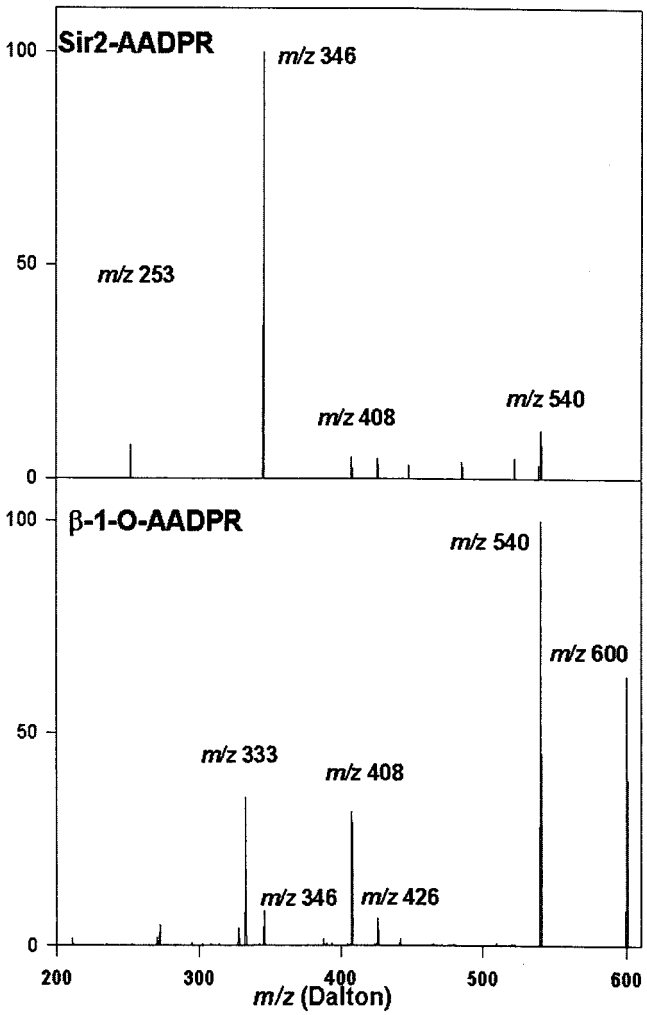

FIGURE 3: Comparative MS/MS spectra of SIR2-derived AADPR and β-1′-AADPR under identical experimental conditions.

molecular ions had the predicted AADPR mass of 600 (*m*/*z*, negative mode) and that both had identical fragmentation patterns (MS/MS). These results indicate that the products of SIR2 are the 2′ and 3′ regioisomers of AADPR (see Methods).

Identification of 2′- and 3′-AADPR Isomers. The identities of 2′- and 3′-AADPR isomers were confirmed by 2D NMR experiments (COESY and NOESY) on HPLC-purified SIR2-derived AADPR (NMR spectra were obtained at 0 °C in 10% methanol-d_4, 90% D_2O). These spectra demonstrated that the major isomer formed in the SIR2 reaction is the 3′ isomer on the basis of a set of complete COESY cross-peaks and a NOE between the acetyl methyl group and the peak assigned to H3′. The HPLC-purified 3′ isomer converted spontaneously to the 2′ isomer and reached a 67:47 equilibrium. The minor isomer formed by the SIR2 reaction was the 2′ isomer, and it was characterized in a sample containing both 2′ and 3′ isomers. The 2′ assignment was made with a COESY assignment and an NOE between the peak of the acetyl methyl and the peak of H2′ (see supplementary data on the website http://www.bioc.aecom.yu.edu/labs/girvlab/nmr/DATA/figure_1droe.jpeg).

NMR and HPLC methods demonstrated an interconversion of 3′ isomers to 2′ isomers with a first-order rate constant for acetyl migration (3′-AADPR → 2′AADPR) of 0.32 h^{-1} at pH 6.25 (Figure 4). The equilibrium constant of K_{eq} was found to be 1.4 at 15 °C, on the basis of HPLC peak integrations of the 2′ and 3′ isomers, and the rate constant for 2′-AADPR → 3′-AADPR is 0.45 h^{-1}. The equilibrium and kinetic description of acetyl migration including the equilibria for the anomeric forms is shown in Figure 1B.

Table 1: Mass Spectrometry: Observed Species in the Presence of ^{18}O and ^{16}O Water[a]

reaction conditions	quench conditions	molecular species (*m*/*z*)	fragmentations (major species)
^{16}O	nq	600	540, 346
^{18}O	nq	602	540, 346
^{16}O	^{18}O, H^+	602	542, 346
^{18}O	^{18}O, H^+	604	542, 346
^{18}O	^{16}O, H^+	602	540, 346
ADPR	^{18}O, pH 7.5	558	346
ADPR	^{18}O, H^+	560	346

[a] The reaction conditions for the first five entries reflect Sir2Af2-mediated deacetylation in 50 mM potassium phosphate (pH 7.8) at 55 °C for 30 min with enrichment of the reaction water content (minimal 65%) with the isotope shown. The reaction was subsequently analyzed by LC/MS in MS and MS/MS modes. The molecular species reflects the observed major ion identified at 7 min, the retention time of AADPR in LC. Fragmentations are based upon MS/MS spectra derived from the selection of the major molecular ion. Not quenched (nq) reflects an injection of otherwise untreated reaction mixtures. In cases where a quench was used, 2 volumes of either 95% $H_2{}^{18}O$ or unlabeled water containing 10% acetic acid-d_4 was added to reaction mixtures after an initial 55 °C incubation period and reacted for 3 h at room temperature. Samples were subsequently analyzed by LC/MS and MS/MS. The bottom two cases reflect the behavior of ADPR in either 50 mM potassium phosphate (pH 7.5) or 95% $H_2{}^{18}O$ containing 10% acetic acid-d_4 after incubation for a 3 h period at room temperature.

Kinetic Sequence of SIR2 Production of the 2′ and 3′ Isomers. An NMR experiment at 5 °C established that 2′-AADPR forms early in the SIR2 reaction followed by the production of the 3′ isomer (Figure 5). Thus, the kinetic sequence for the products is 2′-AADPR before 3′-AADPR (Figure 1C). The rate of SIR2 catalysis exceeds the rate constant for the 2′ → 3′ interconversion with a ratio $k_{cat}/k_{2'\rightarrow 3'}$ of 20 at 5 °C.

Incorporation of $H_2{}^{18}O$ into Product. Reaction stoichiometry for SIR2 (Figure 1C) indicates that two new oxygen atoms are incorporated into AADPR. It has been assumed but not shown that one or more of these oxygen atoms comes from water (*14*, *16*, *18*). Reactions in ^{18}O water followed by an MS analysis of the AADPR product indicated that the product mass is increased by 2 amu, indicating an uptake of a single ^{18}O from water into AADPR. The ^{18}O enrichment (65%) was the same as the ^{18}O content in the water (Figure 5, inset). Dilution of reaction samples in 2 volumes of ^{16}O water at pH 7.5 or in 10% acetic acid-d_4 followed by MS analysis showed that the ^{18}O content did not change over a 24 h period (Table 1). The ^{18}O incorporated is a non-exchangeable oxygen atom under these conditions.

The ^{18}O atom could reside in the acetate moiety or in the 1′-OH of the 2′- and 3′-AADPR molecules. Incubation of ADPR or 2′- and 3′-AADPR in ^{18}O in 10% acetic acid-d_4 (3 h, 25 °C) increased the product mass by 2 amu, indicating an exchange of a single ^{18}O into the product (Table 1). This acid-catalyzed exchange also incorporates a second ^{18}O into AADPR, labeled with $H_2{}^{18}O$ in the SIR2 reaction (Table 1 and Figure 5, inset). Only the 1′-OH group will exchange under these conditions. Therefore, the ^{18}O from the SIR2 reaction is in the acetate moiety, and that exchanged in acid

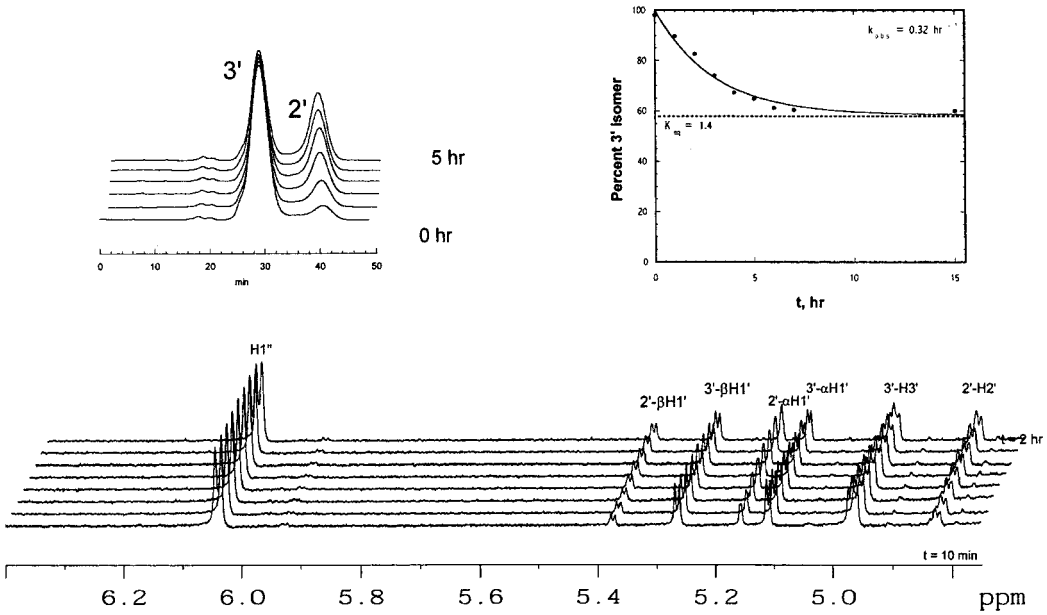

FIGURE 4: (Upper left panel) Time dependence of HPLC chromatograms showing conversion of purified 3′-AADPR to the 2′-AADPR isomer over 5 h at 15 °C. (Lower panel) Stack plot of 1D ^{1}H NMR spectra showing time-dependent conversion of HPLC purified α- and β-3′-AADPR (major) to the α- and β-2′-AADPR (minor) regioisomer as a function of time at 10 °C. (Upper right panel) Plot of 3′-AADPR as a function of time at 15 °C, as measured by HPLC. 3′-AADPR was purified away from the 2′-isomer just prior to incubation. The solid curve represents a best fit to the first-order function as described in the text. The dotted line represents the equilibrium determined by the integration of HPLC peak areas after a 24 h incubation period.

and ^{18}O water is in the 1′-OH group, demonstrating the presence of a free 1′-hydroxyl group in the product.

Exchange experiments were combined with MS/MS studies and reinforced this chemical interpretation (Table 1). Acid-catalyzed exchange reactions of 2′- and 3′-AADPR in ^{18}O water gave a 542 amu fragment, consistent with incorporation of a single ^{18}O into the ribose moiety. Reactions of SIR2 run in either ^{16}O or ^{18}O water led to 540 amu fragments that originated from the loss of acetate. Thus, the nonexchangeable ^{18}O atom obtained from the solvent is incorporated into the carbonyl oxygen of 2′- and 3′-acetates.

Ara-F−NAD$^+$ Is Neither a Substrate Nor an Inhibitor of SIR2. *Ara*-F−NAD$^+$ is a powerful inhibitor for many retaining ADP-ribosyl transfer enzymes (*26*), because the presence of fluorine instead of OH on the 2′ carbon makes *ara*-F−NAD$^+$ approximately 50 times more stable than NAD$^+$ and permits the chemical trapping of enzyme−ADP-ribose covalent intermediates (*27*). *ara*-F−NAD$^+$ did not serve as a substrate, inhibitor, or inactivator of deacetylation or exchange reactions. Thus, the SIR2 reaction mechanism differs from the retaining ADP-ribosyl transferases.

DISCUSSION

Functions of SIR2. Histone deacetylation by SIR2 is proposed to be the major reaction that converts chromatin from active to silent states (*9*, *10*, *12*). This suggestion is supported by studies of silencing complexes which show the SIR2 protein is the only conserved SIR family member found in all of the yeast silencing complexes studied (*28*). Caloric restriction upregulates SIR2 activity and may extend lifespan, showing that silencing might have potent biological effects in various organisms (*29*, *30*). The requirement for NAD$^+$ and evidence that silencing factors can "sense" the redox state of the cell suggests that SIR2 family members are unique amide-hydrolysis enzymes with broad roles (*12*, *31*).

The distribution of the SIR2 family of enzymes into organisms without histone substrates, and eukaryotic genomes encoding multiple Sir2 proteins, suggests a family of deacetylases with varying substrates. Mutagenesis experiments suggest that the N- and C-terminal regions flanking the catalytic core domain of SIR2 help direct it to different targets (*32*). Although most Sir2 proteins in eukaryotic cells are located in the nucleus (*33*), others are cytosolic (*34*−*36*) or even mitochondrial (Onyango, P., Celic, I., Boeke, J. D., and Feinberg, A. P., Unpublished observations) which suggests additional substrates.

Product of SIR2. The identification of 2′-AADPR as the product of SIR2 deacetylation established SIR2s as unique NAD$^+$-dependent enzymes. The product of SIR2 is not β-1′-AADPR, as suggested from the precedent of other ADP-ribosyl transferases that also catalyze nicotinamide exchange reactions (*15*−*17*). Both NAD$^+$ glycohydrolases and CD38 form products with a β configuration and catalyze base-exchange reactions. The synthesis of authentic β-1′-AADPR and the comparison to Sir2 AADPR established that none of the acetyl product formed by SIR2 is this compound. The solution stability observed for β-1′-AADPR further established that it is not an intermediate in the SIR2 reactions. The product released from the catalytic site of SIR2 is 2′-AADPR, which forms a SIR2-independent equilibrium of 2′- and 3′-acetyl isomers. The acetyl exchange results in a nearly equal ratio of isomers that equilibrate within an hour at physiological temperatures of 37 °C. It is possible that a downstream action of SIR2 could be timed by the isomerization of 2′- to 3′-AADPR. Both regioisomers exist in α- and β-1′-anomeric forms, generating four distinct species by NMR (Figure 1B). The α/β anomeric equilibrium is fast (>50 s^{-1}).

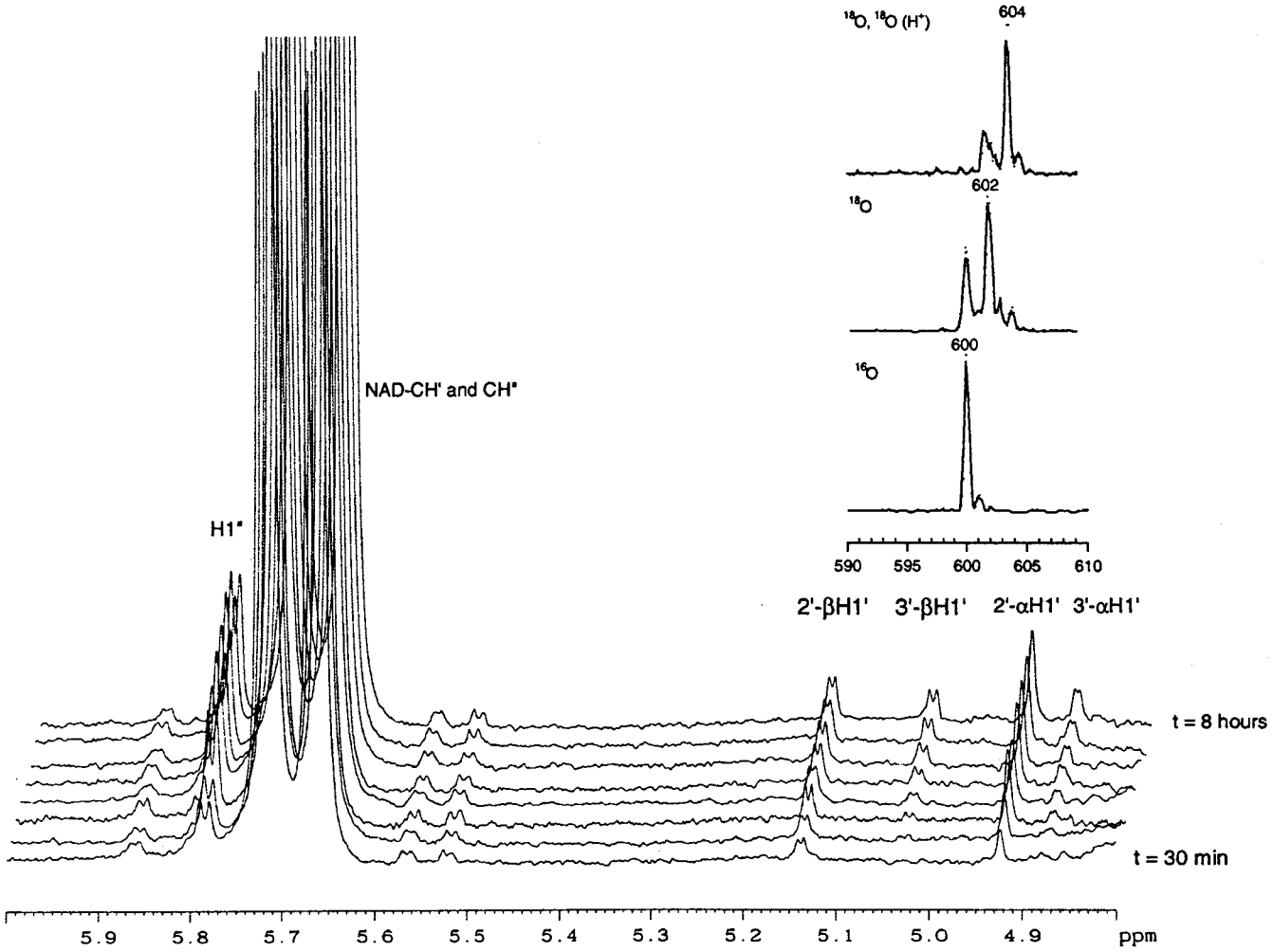

FIGURE 5: Stack plot of 1D ^{1}H NMR spectra (600 MHz) taken at 5 °C, showing the initial formation of 2′-AADPR (resonances at $\delta = 5.15$ (2′β) and 4.93 (2′α)) catalyzed by 50 μM Sir2Af2 in the presence of 10 mM NAD^+ and 1.5 mM JB12 peptide. Later time points illustrate the conversion of 2′-ADPR to 3′-ADPR (resonances at $\delta = 5.04$ (3′β) and 4.88 (3′α)). Spectra are separated in time by 1.0 h. (Inset) MS spectra of molecular ions of AADPR derived from Sir2Af2 reactions after treatment with isotope-labeled water in reaction or in quench. Top panel shows ions derived from a Sir2Af2 reaction in ^{18}O water followed by a $H_2{}^{18}O$ quench containing 10% acetic acid-d_4 for 3 h at room temperature. Middle panel shows ions derived from the Sir2Af2 reaction in ^{18}O water without quenching. Bottom panel shows ions derived from the Sir2Af2 reaction in unlabeled water without quenching. Results for other conditions and experimental details are listed in Table 1 and the legend.

SIR2-Catalyzed Steps That Generate 2′-AADPR. The formation of 2′-AADPR requires that the 2′-hydroxyl acts as a nucleophile at some stage of the chemical mechanism. The 2′-hydroxyl has been proposed to act directly as the nucleophile to deacetylate the amide moiety (*16*). However, this mechanism requires the incorporation of ^{18}O from solvent water at the 1′ position as the sole ^{18}O label in the 2′-AADPR released from SIR2. Analysis by MS established that ^{18}O appeared in the acetyl group; therefore, action of the 2′-hydroxyl group as the primary nucleophile could be eliminated. The single water molecule mechanism and an acid-exchangeable oxygen at the C1′-hydroxyl confirm an acyl-oxygen−C1′ bond formation and the attack of water at the carbon of the amide carbonyl.

Enzymes catalyzing ADP-ribosyl transfer reactions generate highly reactive ADP-ribooxacarbenium ions that can be attacked by weak nucleophiles. For example, in cholera toxin, ADPR is transferred from NAD^+ to an arginine with stereochemical inversion of the ADP ribose to generate an α-1′-substituted ADPR amidate (*37*). Transition-state studies of all ADP-ribose transfer reactions thus far characterized show that a highly reactive ribooxacarbenium ion electrophile is generated to facilitate ADPR transfer chemistry (*38*). This same strategy in the SIR2 reaction generates an ADP-ribooxacarbenium ion that captures the acyl oxygen of *N*-acetyl lysine to generate an *O*-alkyl amidate (Figure 1D). *O*-Alkyl amidates hydrolyze spontaneously in water to form free amines and esters (*39*). For SIR2, this hydrolysis would form deacetylated lysine and α-1′-AADPR.

Only two reaction pathways can form 2′-AADPR. In the first, the intermediate *O*-alkyl amidate hydrolyzes to a 1′-substituted α-AADPR that isomerizes to a 2′ regiochemistry to give the observed product (Figure 1D). Alternatively, the 2′-hydroxyl could attack the *O*-alkyl amidate intermediate to generate a cyclic acyloxonium, followed by hydrolysis to form the observed 2′-AADPR product (Figure 1E). These mechanisms explain the requirement of the peptide substrate to permit nicotinamide $\rightleftharpoons NAD^+$ exchange, even in mutagenized enzymes that lack deacetylase activity (*18*).

Nature of the α-1′-Intermediate. Low-temperature NMR studies performed at 5 °C using Sir2Af2 furnished no evidence for accumulation of an α-1′-intermediate. Therefore,

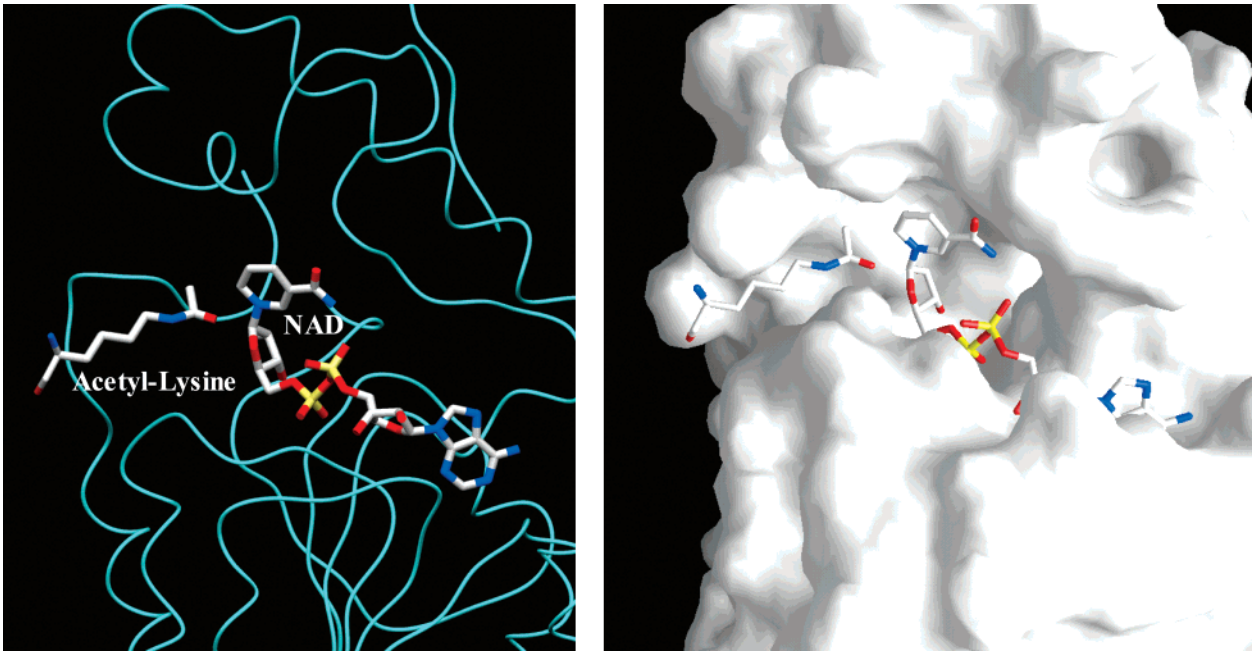

FIGURE 6: Acetyl lysine side-chain docked into the active-site cavity of Sir2 (*18*). Right and left panels are peptide-backbone and space-filling models, respectively. The acetyl-oxygen is within van der Waals contact of C1′ of NAD^+. The acetyl moiety can be placed in the proper attack geometry to form an acyl-O−C1′ bond with α stereochemistry.

any discrete intermediate must convert to 2′-AADPR more rapidly than the catalytic rate of the enzyme, because the detection level for an α-1′-intermediate was near the enzyme concentration. The 2′- to 3′-AADPR interconversion is slower than k_{cat} by a factor of 20, and the enzyme-dependent production of the 2′ isomer was observed by NMR (Figure 5). Transient formation of α-1′-AADPR is unfavorable based on nicotinamide exchange, and the preferred mechanism is formation of the 1′-*O*-alkylamidate intermediate, followed by the 2′-hydroxyl attack to form a 1′,2′-substituted acyl-oxonium structure as the precursor to 2′-AADPR formation on the enzyme (Figure 1E).

X-ray Structure Is Consistent with the Mechanism and Observed Products. The SIR2 X-ray structure with bound NAD^+ establishes that there are no nucleophilic residues near the C1′ of NAD^+ to support a covalent ADPR transfer and a formation of *β*-1′-AADPR as the stereochemical outcome (*18*). A view of the structure with knowledge of the α-1′-intermediate indicates that the α face of NAD^+ is available for attack by a bound acetyl lysine and that the 2′-hydroxyl is free to serve as a nucleophile. The crystal structure of Sir2 permits facile docking of an acetyl lysine residue into the catalytic site (Figure 6). The acetyl oxygen can be positioned for an optimal approach to the α face of the NAD^+ bound to Sir2. Histidine116 adjacent to the 3′-hydroxyl has been shown by mutagenesis to be essential for deacetylase function, also indicating that the α-face of the NAD^+ ribosyl group is the site of acid−base transfer pathways for catalytic function.

A catalytic role for His116 can be proposed from X-ray studies (*18*; Figure 7). The nucleophilic 2′-OH is activated through a proton relay via the 3′-OH in which the histidine serves as the ultimate proton acceptor. The early involvement of the 2′-OH as a nucleophile in the catalytic mechanism, in direct attack upon the amide (Figure 7, part A), requires the direct coupling of 2′-OH activation and nicotinamide exchange. Mutagenesis studies show that the replacement of His for Ala in the HST2-SIR2 homologue abrogates deacetylation but leaves intact 25% of the wild-type nicotinamide exchange activity (*18*). This result strongly supports the exchange mechanism and reaction coordinate suggested in Figure 1E and part B of Figure 7, where the 2′-OH activation occurs downstream from the nicotinamide exchange reaction and permits enzymatic decoupling of exchange and deacetylation.

Summary of the SIR2 Mechanism. The sum of these results provides support for the reaction steps in Figure 1E. Most histone deacetylases are simple hydrolases, because the hydrolysis of *N*-acetyl groups is a chemically simple and energetically favorable reaction. A biological rationale for the consumption of metabolically valuable NAD^+ as a cosubstrate may include substrate signaling in which NAD^+ levels signal cellular energetic and redox states to control SIR2-based gene regulation. A second possibility is that SIR2 initiates a signal transduction pathway by generation of the novel compounds 2′- and 3′-AADPR. These molecules have not been previously recognized in metabolism and carry the features of metabolic instability common to other initiators of signaling pathways. It is conceivable that a cascade of biological events downstream of SIR2 action could be influenced by the isomerization of 2′- to 3′-AADPR. Recent evidence that some SIR2 homologues are cytosolic (*35*, *36*) and can accept acetyl groups from other nonhistone proteins, such as chemically acetylated BSA (*18*) or p53, suggest an expanded role in cell development and transcriptional regulation. Identification of the products of SIR2 provides access to further investigations of these pathways and provides information for inhibitor design for this unusual ADP-ribosyl transferase.

METHODS[2]

Enzyme Assays. Sir2 enzymes were purified as GST fusions (*19*). Peptides JB11 (HSSHLKSKKGQSTSRHKK)

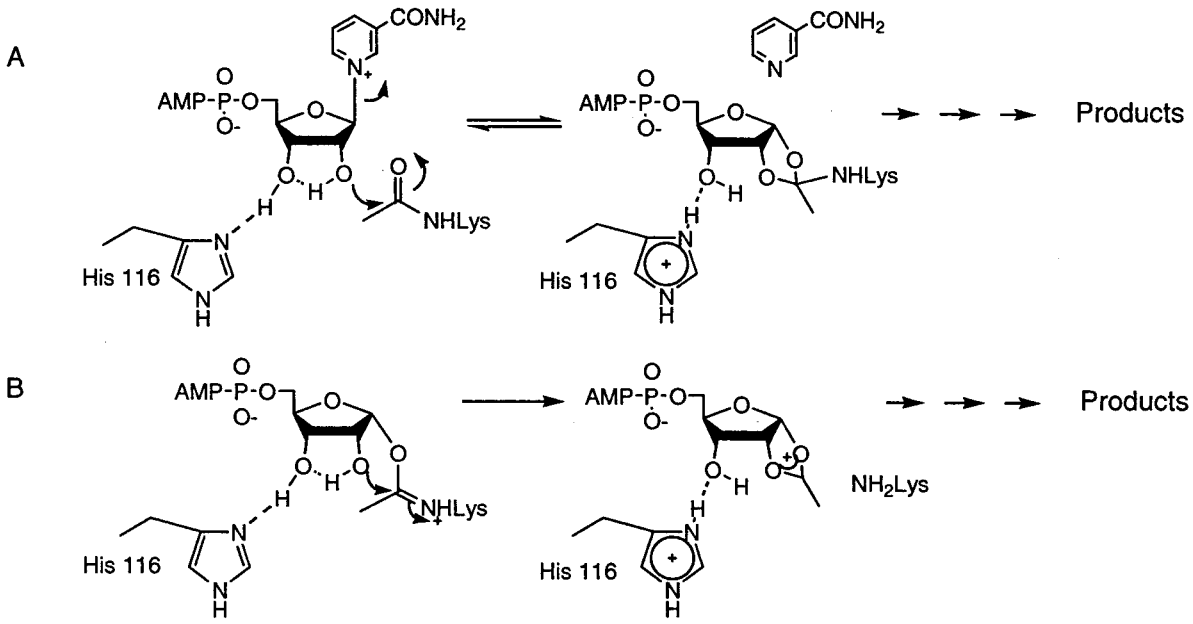

FIGURE 7: (A) Deacetylation mechanism initiated by 2′-OH nucleophilic attack of the amide carbonyl of an acetyl lysine residue. Mechanism A is unlikely because mutation of His to Ala would eliminate nicotinamide exchange. His116 ligated to 3′-OH acts as a base catalyst to activate 2′-OH through a proton-transfer relay mechanism via 3′-OH. (B) Deacetylation mechanism dependent upon the breakdown of 1′-*O*-amidate by 2′-OH attack, downstream from nicotinamide bond cleavage. Mechanism B permits nicotinamide exchange prior to 2′-OH activation, consistent with the exchange reported for the His to Ala mutant (see text).

and JB12 (KKGQSTSRHKKAcLMFKTEG) were based upon the C terminus of p53 at sites known to be acetylated in vivo (*20*−*23*). Native human p53 protein acetylated in vitro by p300 was shown to be an in vitro substrate for Sir2Af2, Sir2A, and yeast Sir2 protein (I.C., and J.D.B. Unpublished data). The peptides were synthesized by the Johns Hopkins Medical Institutions Sequencing and Synthesis Facility and purified by HPLC before use. Peptides were assayed for deacetylation by HPLC as follows. Peptide JB12D (deacetyl version) was made as a standard and comigrated with the JB12 product peak. For peptides JB11 and JB12, 100 μg of peptide was incubated with 10 μg of GST-Sir2p and 200 μM NAD overnight at 30 °C in 50 mM Tris-Cl (pH 8.0) and 50 mM NaCl. The molecular masses of the substrate and product peaks were determined (JB11 = 2104.5, product = 2061.6; JB12 = 2137.2; product = 2094.3). The same reaction conditions were used for Sir2Af2, TmSir2 (eubacterial *Thermotoga maritima*), and GST-Sir2A (human recombinant) (*19*). Incubation was at 55 °C for Sir2Af2 and TmSir2 and at 37 °C for GST-Sir2A. HPLC fractions (500 μl) were analyzed by MALDI−TOF spectrometry. All of these enzymes formed AADPR and deacetylated JB11 and JB12 peptides.

Synthesis of β-1′-AADPR. To 100 mg of NAD^+ in 5 mL of 4 M NaOAc (pH 6.5) was added 50 μg of CD38 enzyme (*27*) dissolved in 50 mM NaOAc (pH 5.0). After overnight incubation at 37 °C, the material was filtered (Millipore Biomax 10 K NMWL, Bedford, MA), injected, and purified by HPLC (0.5% TFA eluant). A peak eluting before NAD^+ (40 versus 50 min, respectively) was collected and lyophilized. The product (yield 28%) was characterized by MS and NMR and determined to be β-1′-AADPR.

[2] General methods, tabulated ^{1}H NMR data of AADPR compounds, and *ara*-F−NAD^+ assays can be found in the Supporting Information.

Purification of 3′-AADPR and NMR Characterization. Sir2Af2 products for NMR analysis were obtained by incubation (40 °C overnight) of 300 μg of Sir2Af2 enzyme, 20 mg of NAD^+, and 70 mg of JB12 peptide in 5 mL of a 40 mM potassium phosphate buffer (pH 6.25). The mixture was filtered (Millipore Biomax 10K NMWL) and loaded onto DEAE A-50 columns (1 mL) equilibrated with 25 mM NaOAc (pH 6.0). Elution with 2, 3, and 2 mL of 250 mM, 500 mM, and 1 M NaOAc (pH 6.0), respectively, gave a fractionation of products. The last fractions contained AADPR and were separated on a semipreparative C-18 column eluted with 1 mM KPO_4 (pH 5.0) at 2 mL/min (5 mL injection volume). The 3′-AADPR eluted at 14 min and was evaporated to dryness at 2 °C under high vacuum. This material was kept ice-chilled in D_2O until ^{1}H NMR spectra were taken. The 1D and 2D COESY and NOESY experiments provided assignment of 3′-AADPR and showed conversion to 2′-AADPR.

Purification of 2′-AADPR and NMR Characterization. The 2′-AADPR isomer eluted as the second peak in the HPLC chromatogram described previously. HPLC (50 mM NH_4-AcO (pH 5.0)) showed that 2′-AADPR converts readily to the 3′-AADPR. 2′-AADPR was characterized in the equilibrium mixture with 3′-AADPR at a 47:67 ratio (2′-AADPR/3′-AADPR) by HPLC. ^{1}H NMR data allowed for full characterization.

Interconversion Rates of 2′- and 3′-AADPR. A sample of 3′-AADPR was incubated at 15 °C in 25 mM KPO_4 (pH 6.25) and assayed by HPLC at 40 min intervals (C-18, 50 mM NH_4AcO (pH 5.0)). The percentage of 3′ isomer was fit to the equation 3′-AADPR (%) = $P_a \exp(-kt) + P_f$, where $P_a + P_f = P_0$ (P_a is the percentage of the 3′-isomer above equilibrium at $t = 0$, t is time, k is the first-order rate constant, P_f is the equilibrium percentage, and P_0 is the initial percentage).

Low-Temperature Studies of Sir2Af2. A total of 1.7 mg of Sir2Af2 and 2 mg of JB12 peptide (95% D_2O, 50 mM K_2PO_4H (pH 6.3), 550 μL) were cooled to 5 °C in a 600 MHz NMR spectrometer. Initial spectra were obtained, and 280 μL of chilled 22 mM NAD^+ was added to initiate the reaction. ^1H NMR spectra were obtained at intervals over 18 h at 5 °C.

$H_2{}^{18}O$ Incorporation into 2′- and 3′-AADPR. Reactions of 2 μg of Sir2Af2, 100 μg of JB12, and 300 μM NAD^+ in 200 μL of $H_2{}^{18}O$ (94.5%, containing 40 mM $K_2PO_4H_2$ (pH 7.5)) were incubated at 55 °C and assayed by C-18 LC/MS in negative-ion mode (eluant: 0.5% formic acid). The peptide, NAD^+, ADPR, and AADPR were resolved. Ions of AADPR in ^{18}O incubations versus ^{16}O controls showed a 2 amu mass increase (602 versus 600), indicating a single ^{18}O incorporation. MS/MS spectra of both ^{16}O and ^{18}O AADPR included a major fragmentation at $m/z = 540$ due to the loss of $HOOCCH_3$ and $HO^{18}OCCH_3$, respectively. MS spectra of purified 2′- or 3′-AADPR from reactions were identical. Sir2 reactions ($H_2{}^{16}O$ or $H_2{}^{18}O$) or ADPR were quenched with 2 volumes of $H_2{}^{16}O$ or $H_2{}^{18}O$ in 10% acetic acid-d_4. LC/MS and MS/MS data are shown in Table 1.

ACKNOWLEDGMENT

We thank Drs. C. Grubmeyer for initiating this collaboration, C. Wolberger for discussions, and R. Cole for MS assistance at Johns Hopkins (an NIH Research Resource). The work was supported by NIH grants GM62385 (J.D.B.) and AI34342 (V.L.S.).

NOTE ADDED IN PROOF

The action of SIR2 on p53 has recently been reported for both in vitro and in vivo systems (*40*, *41*), consistent with the reactions reported here with p53 peptides.

SUPPORTING INFORMATION AVAILABLE

General methods, tabulated ^1H NMR data of AADPR compounds, and *ara*-F−NAD^+ assays. This material is available free of charge via the Internet at http://pubs.acs.org.

REFERENCES

1. Brachmann, C. B., Sherman, J. M., Devine, S. E., Cameron, E. E., Pillus, L., and Boeke, J. D. (1995) *Genes Dev. 9*, 2888−90.
2. Frye, R. A. (1999) *Biochem. Biophys. Res. Commun. 260*, 273−9.
3. Moretti, P., Freeman, K., Coodly, L., and Shore, D. (1994) *Genes Dev. 8*, 2257−69.
4. Rine, J., and Herskowitz, I. (1987) *Genetics 116*, 9−22.
5. Shou, W., Seol, J. H., Shevchenko, A., Baskerville, C., Moazed, D., Chen, Z. W., Jang, J., Charbonneau, H., and Deshaies, R. J. (1999) *Cell 97*, 233−44.
6. Straight, A. F., Shou, W., Dowd, G. J., Turck, C. W., Deshaies, R. J., Johnson, A. D., and Moazed, D. (1999) *Cell 97*, 245−56.
7. Hecht, A., Laroche, T., Strahl-Bolsinger, S., Gasser, S. M., and Grunstein, M. (1995) *Cell 80*, 583−92.
8. Johnson, L. M., Kayne, P. S., Kahn, E. S., and Grunstein, M. (1990) *Proc. Natl. Acad. Sci. U.S.A. 87*, 6286−90.
9. Braunstein, M., Rose, A. B., Holmes, S. G., Allis, C. D., and Broach, J. R. (1993) *Genes Dev. 7*, 592−604.
10. Imai, S., Armstrong, C. M., Kaeberlein, M., and Guarente, L. (2000) *Nature 403*, 795−800.
11. Landry, J., Sutton, A., Tafrov, S. T., Heller, R. C., Stebbins, J., Pillus, L., and Sternglanz, R. (2000) *Proc. Natl. Acad. Sci. U.S.A. 97*, 5807−11
12. Smith, J. S., Brachmann, C. B., Celic, I., Kenna, M. A., Muhammad, S., Starai, V. J., Avalos, J. L., Escalante-Semerena, J. C., Grubmeyer, C., Wolberger, C., and Boeke, J. D. (2000) *Proc. Natl. Acad. Sci. U.S.A. 97*, 6658−63.
13. Tsang, A. W., and Escalante-Semerena, J. C. (1998) *J. Biol. Chem. 273*, 31788−94.
14. Landry, J., Slama, J. T., and Sternglanz, R. (2000) *Biochem. Biophys. Res. Commun. 278*, 685−90.
15. Tanner, K. G., Landry, J., Sternglanz, R., and Denu, J. M. (2000) *Proc. Natl. Acad. Sci. U.S.A. 97*, 14178−82.
16. Tanny, J. C., and Moazed, D. (2001) *Proc. Natl. Acad. Sci. U.S.A. 98*, 415−20.
17. Moazed, D. (2001) *Curr. Opin. Cell Biol. 13*, 232−8.
18. Min, J., Landry, J., Sternglanz, R., and Xu, R. M. (2001) *Cell 105*, 269−79.
19. Smith, J. S., Avalos, J., Celic, I., Muhammad, S., Wolberger, C., and Boeke, J. D. (2001) *Methods Enzymol. 342*, in press.
20. Gu, W., and Roeder, R. G. (1997) *Cell 90*, 595−606.
21. Abraham, J., Kelly, J., Thibault, P., and Benchimol, S. (2000) *J. Mol. Biol. 295*, 853−64.
22. Liu, L., Scolnick, D. M., Trievel, R. C., Zhang, H. B., Marmorstein, R., Halazonetis, T. D., and Berger, S. L. (1999) *Mol. Cell. Biol. 19*, 1202−9.
23. Sakaguchi, K., Herrera, J. E., Saito, S., Miki, T., Bustin, M., Vassilev, A., Anderson, C. W., and Appella, E. (1998) *Genes Dev. 12*, 2831−41.
24. Sterner, D. E., and Berger, S. (2000) *Microbiol. Mol. Biol. Rev. 64*, 435−59.
25. Cervantes-Laurean, D., Jacobson, E. L., and Jacobson, M. K. (1997) *Methods Enzymol. 280*, 275−87.
26. Muller-Steffner, H. M., Malver, O., Hosie, L., Oppenheimer, N. J., and Schuber, F. (1992) *J. Biol. Chem. 267*, 9606−11.
27. Sauve, A. A., Deng, H. T., Angeletti, R. H., and Schramm, V. L. (2000) *J. Am. Chem. Soc. 122*, 7855−7859.
28. Gottschling, D. E. (2000) *Curr. Biol. 10*, R708−11.
29. Lin, S. J., Defossez, P. A., and Guarente, L. (2000) *Science 289*, 2126−8.
30. Tissenbaum, H. A., and Guarente, L. (2001) *Nature 410*, 227−30.
31. Guarente, L. (2000) *Genes Dev. 14*, 1021−6.
32. Cuperus, G., Shafaatian, R., and Shore, D. (2000) *EMBO J. 19*, 2641−51.
33. Gotta, M., Strahl-Bolsinger, S., Renauld, H., Laroche, T., Kennedy, B. K., Grunstein, M., and Gasser, S. M. (1997) *EMBO J. 16*, 3243−55.
34. Afshar, G., and Murnane, J. P. (1999) *Gene 234*, 161−8.
35. Perrod, S., Cockell, M. M., Laroche, T., Renauld, H., Ducrest, A. L., Bonnard, C., and Gasser, S. M. (2001) *EMBO J. 20*, 197−209.
36. Yang, Y. H., Chen, Y. H., Zhang, C. Y., Nimmakayalu, M. A., Ward, D. C., and Weissman, S. (2000) *Genomics 69*, 355−69.
37. Rising, K., and Schramm, V. L. (1997) *J. Am. Chem. Soc. 119*, 27−37.
38. Scheuring, J., Berti, P. J., and Schramm, V. L. (1998) *Biochemistry 37*, 2748−58.
39. Borch, R. F. (1968) *Tetrahedron Lett. 1*, 61−65.
40. Vaziri, H., Dessain, S. K., Eaton, E. N., Imai, S.-I., Frye, R. A., Pandita, T. K., Guarente, L., and Weinberg, R. A. (2001) *Cell 107*, 149−159.
41. Luo, J., Nikolaev, A. Y., Imai, S.-I., Chen, D., Su, F., Shiloh, A., Guarente, L., and Gu, W. (2001) *Cell 107*, 137−148.

BI011858J